5-26-1961

Shock-Tube Determination of Dissociation Rates of Oxygen

John P. Rink

SHOCK TUBE DETERMINATION OF DISSOCIATION RATES OF OXYGEN ▪ RINK

SHOCK TUBE DETERMINATION OF DISSOCIATION RATES OF OXYGEN

by

John P. Rink

A Thesis
Submitted in Partial Fulfillment of the
Requirements for the Degree of
Master of Science in Physics

The University of New Mexico
1961

This thesis, directed and approved by the candidate's committee, has been accepted by the Graduate Committee of the University of New Mexico in partial fulfillment of the requirements for the degree of

MASTER OF SCIENCE

E F Castetter
Dean

May 26, 1961
Date

Thesis committee

Russell E. Duff
Chairman

Walter M. Elsasser

[illegible]

ACKNOWLEDGMENTS

The author takes pleasure in acknowledging the invaluable aid received from Dr. Russell E. Duff, Dr. Herbert T. Knight, and Dr. Garry L. Schott. The author is indebted to Richard E. Johnston for his help in performing the experiments.

I also want to express appreciation to the Atomic Energy Commission and the University of California for the use of their facilities and equipment at the Los Alamos Scientific Laboratory.

ACKNOWLEDGMENTS

The author takes pleasure in acknowledging the invaluable aid received from Dr. Russell [illegible], Dr. [illegible], and Dr. Gerry L. Schott. The author is indebted to [illegible] for his help in performing the experiment.

I also want to express appreciation to the Atomic Energy Commission and the University of California for the use of their facilities and equipment at the Los Alamos Scientific Laboratory.

TABLE OF CONTENTS

TABLE OF CONTENTS

List of Figures

List of Tables

ABSTRACT

The rate of dissociation of oxygen in Xe-O_2 mixtures was measured over a temperature range of 3000°K to 6000°K. An x ray densitometer was used to measure the density during the dissociation process behind a shock wave. It was possible to match the experimental data with theoretical density profiles over a wide range of compositions and initial conditions. The reactions considered were

$$O_2 + M \underset{k_r}{\overset{k_d}{\rightleftharpoons}} 2\,O + M,$$

where M can be Xe, O_2, or O. Considering these species as third bodies, the measured recombination rates in $cc^2 mole^{-2} sec^{-1}$ were $4.7 \times 10^{17}\ T^{-1}$, $1.6 \times 10^{18}\ T^{-1}$, and $4.8 \times 10^{18}\ T^{-1}$ respectively. The third body efficiencies of O_2 and O relative to Xe are 3 and 10. Experimental conditions were such that an accurate measurement of the exponent of the temperature could not be made. However, since the data showed it to be within the limits of -1/2 and -2, a value of -1.0 was arbitrarily chosen. The agreement between results reported here and previous work demonstrates the potential utility of this method for kinetic studies of other reactions.

ABSTRACT

The rate of dissociation of oxygen in Ar-O_2 mixtures was measured over a temperature range of 3000°K to 6000°K. An x-ray densitometer was used to measure the density during the dissociation process behind a shock wave. It was possible to match the experimental data with theoretical density profiles over a wide range of compositions and initial conditions. The reactions considered were

$$O_2 + M \underset{k_r}{\overset{k_d}{\rightleftharpoons}} 2O + M$$

where M can be Ar, O_2, or O. Considering these species as third bodies, the measured recombination rates in [illegible] were [illegible] $\times 10^{[illegible]}$ T[illegible], [illegible] $\times 10^{[illegible]}$ T[illegible] and [illegible] $\times 10^{[illegible]}$ T[illegible] respectively. The third body efficiencies of O_2 and O relative to Ar are [illegible] and [illegible]. Experimental conditions were [illegible] that [illegible] of the temperature could not be found. However, since the data showed it to be within the limits of -1.5 and +2, a value of -1.0 was arbitrarily chosen. The [illegible] between results reported here and previous work demonstrates the potential ability of this method for kinetic studies of other reactions.

SHOCK TUBE DETERMINATION OF DISSOCIATION RATES OF OXYGEN

I. Introduction

This study has a two-fold purpose--to demonstrate the feasibility of using x ray densitometry of shock waves to determine chemical reaction rates and to obtain an accurate, independent measurement of the dissociation rate of oxygen. Previous measurements of the dissociation rate of oxygen in shock tubes have employed techniques based on interferometric measurements of density[1,2] and on ultraviolet light absorption to determine oxygen concentration[3,4]. An independent method of determining reaction rates is presented here. Density as a function of time behind a shock wave in Xe-O_2 mixtures was measured by x ray absorption. Then an IBM 704 computer was utilized to calculate a density profile by integrating the simultaneous chemical kinetic equations which describe the system, subject to the appropriate hydrodynamic constraints. The reaction rate coefficients were deduced from the experimental data by obtaining agreement between the measured and calculated density profiles.

[illegible]

[illegible]

This study [illegible]

of using a [illegible]

action rates and [illegible]

dissociation rate [illegible]

rate of oxygen [illegible]

ferometric [illegible]

to determine [illegible]

peroxide [illegible]

of the [illegible]

absorption. [illegible]

[illegible]

equations [illegible]

[illegible]

the experimental [illegible]

calculated [illegible]

Rates have been determined in mixtures of 95% Xe - 5% O_2, 85% Xe - 15% O_2, 50% Xe - 50% O_2, and 30% Xe - 70% O_2 at pre-shock pressures from 9 mm Hg to 30 mm Hg. The temperature range for these experiments was 3000°K to 6000°K.

II. Theoretical Considerations

The equation for the overall rate of change of oxygen concentration at a given condition behind a shock wave in a mixture of Xe and O_2 is

$$(\partial [O_2]/\partial t)_v = -k_{d_1}[O_2][Xe] - k_{d_2}[O_2]^2 - k_{d_3}[O_2][O]$$

$$+ k_{r_1}[O]^2[Xe] + k_{r_2}[O]^2[O_2] + k_{r_3}[O]^3 . \qquad (1)$$

Ozone was not considered as an intermediate in the dissociation process since it has been shown to be unimportant under the conditions of this experiment[4,5]. If rotational and vibrational equilibrium are assumed, one can say that the rate coefficients in Eq. 1 are related to K, the equilibrium constant, by

$$K = k_{d_1}/k_{r_1} = k_{d_2}/k_{r_2} = k_{d_3}/k_{r_3} \qquad (2)$$

Glick and Wurster[6] and Losev[4] have observed a separation between vibrational relaxation and the O_2 dissociation process in a shock tube. Camac and Vaughan[3] have made a similar observation at temperatures below 8000°K. Above this temperature they found that the two rates become comparable. Thus the assumption that rotational and vibrational

equilibrium is established before appreciable dissociation occurs appears to be valid, and Eq. 2 should hold for the shock conditions used in this work.

Since the rate coefficients are related by Eq. 2, and the entire course of dissociation from the very early stages to equilibrium is considered in the data analysis, logically either the dissociation or the recombination rate coefficient may be used to define the reaction rate for a given third body. In this paper the rate coefficients are expressed in terms of the recombination rate, k_r, in the form

$$k_{r_i} = A_i \; T^{m_i} \tag{3}$$

The index differentiates between the three possible third bodies as indicated in Eq. 1. The activation energy for the recombination process is assumed to be zero which implies that the activation energy for dissociation is the dissociation energy.

Rate determinations were made by comparing calculated density-distance profiles behind shock waves with those obtained experimentally. the computation of a density vs distance profile was made with an IBM 704 code by Duff. He gives the following description of this code[7]. "Values of temperature, pressure, and volume are determined from the given concentrations and initial data in such a way that the hydrodynamic constraints are satisfied. These values of the thermodynamic variables and concentrations are used to calculate the rate of change of each component with time. The Runge-Kutta integration procedure is then used to determine concentrations for the next cycle. This procedure is repeated until the entire profile is determined."

equilibrium is reached [illegible] before appreciable [illegible] occurs appears to be valid, and Eq. 4 should hold for the shock conditions used in this work.

Since the rate coefficients are related by Eq. 4, and the entire course of dissociation from the very early stages to equilibrium is considered in the data analysis, [illegible] either the dissociation or the recombination rate coefficient may be used to define the reaction rate for a given shock wave. In this paper the rate coefficients are expressed in terms of the recombination rate, k_r, in the form

$$k_r = [illegible] \qquad (5)$$

The [illegible] differences between the three [illegible] is indicated in Eq. 5. The activation energy for the recombination process is assumed to be zero which implies that the activation energy for dissociation is the dissociation energy.

The determinations were made by fitting the calculated density distance profiles [illegible] those obtained experimentally. The computation of a density or distance profile was done with [illegible] code by [illegible]. He gives the following description of this code: "Values of [illegible] temperature, pressure, [illegible] values are determined from the given concentrations and initial data in such a way that the hydrodynamic conservation [illegible] are satisfied. These values of the thermodynamic variables and concentrations are used to calculate the rate of change of each component with time. The Runge-Kutta integration procedure is then used to [illegible] for the next [illegible]. This procedure is repeated until the entire profile is determined."

For these calculations the following data must be supplied: either a dissociation or recombination rate coefficient for each reaction pair considered; the shock velocity; and parameters specifying the state of the gas assuming vibrational and rotational equilibrium but no chemical reaction. These no-reaction parameters of pressure, density, temperature, and particle velocity behind the shock front for a given shock velocity were calculated in the usual way from the conservation laws for mass, momentum, and energy and the perfect gas law. Values of enthalpy and free energy as functions of temperature needed in these calculations were obtained from quartic polynomial fits of the O_2 data of Johnston et al[8] and the NBS tabulation for O atom[9]. The heat of formation of O was assumed to be 58.98 kcal/M[10].

An iterative procedure was used to deduce the k_{r_i} from the experimental density-time profiles. The first step was to derive an approximate Xe rate by fitting the 95% Xe - 5% O_2 data. In this fitting the rates for O_2 and O as third bodies given by Camac and Vaughan[3] were used, and the Xe rate was varied until agreement was obtained. Using this value for the Xe rate and the 30% Xe - 70% O_2 data, new values for the O_2 and O rates were obtained. This cycle was repeated until a consistent set of k_{r_i} was obtained which fit the experimental profiles equally well over the entire experimental range of composition and temperature. The profiles calculated for intermediate compositions lacked sensitivity to variations of a single rate coefficient. However, they were useful as an overall check of the final set of rates.

III. Experimental Procedures

The shock tube and x ray densitometer used for this experiment was originally designed and built by Knight and Venable[11] to measure densities in gaseous detonations. Since its conception there have been many modifications to the shock tube and auxiliary equipment to provide density measurements in shocked gases. A discussion follows of the important apparatus used in this experiment, some of which are unchanged from the original design.

Figure 1 is a block diagram illustrating the physical and electrical relationship of the components along the shock tube. The compression chamber was a cylindrical brass tube 4 ft long and 4 in i.d. It was separated from the steel diaphragm station by a micarta spacer which provided thermal insulation. This chamber was wrapped with eight, equally spaced, 110 v ac heating tapes so that the entire compression chamber could be heated to 100°C. Approximately 15 min was required to heat the compression chamber from room temperature to 100°C.

Heating the driver gas increased its sound speed. All other parameters being the same, this would produce a stronger shock than with unheated gas. This was a device to increase the shock strength while not exceeding the structural limitations of the valves, the thermocouple, and the micarta spacer connected to the compression chamber.

The diaphragm station was built with a circular tongue and groove at a larger diameter than the O-rings that provided the vacuum and pressure seal against the diaphragm itself. This tongue and groove gripped the diaphragm firmly and prevented wrinkling when high pressures

III. EXPERIMENTAL PROCEDURE

The shock tube and x-ray densitometer used for this experiment was originally designed and built by [illegible] and [illegible][1] to measure density [illegible] in gaseous detonations. Since its construction there have been many modifications to the shock tube and auxiliary equipment to provide density measurements in shocked gases. A discussion follows of the important apparatus used in this experiment, some of which are unchanged from the original design.

Figure 1 is a block diagram illustrating the physical and electrical relationship of the components along the shock tube. The compression chamber was a cylindrical brass tube 4 ft long and 4 in i.d. It was separated from the steel expansion section by a diaphragm holder which provided thermal insulation. This chamber was wrapped with eight equally spaced, 110-v ac heating tapes so that the entire compression chamber could be heated to 150°C. Approximately 1½ hr was required to heat the compression chamber from room temperature to 150°C.

Heating the driver gas increases its sound speed. All other parameters being the same, this would produce a stronger shock than with unheated gas. This was a [illegible] to [illegible] the shock strength while keeping the [illegible] [illegible] of the valves, the thermocouple and the pressure gauge connected to the compression chamber.

The diaphragm station was fitted with a circular knife and groove of a larger diameter than the 4-in. tube that provided the increased pressure seal against the diaphragm itself. This design and groove gripped the diaphragm firmly and prevented wrinkling when high pressures

Fig. 1. A block diagram of the physical and electrical connections along the shock tube.

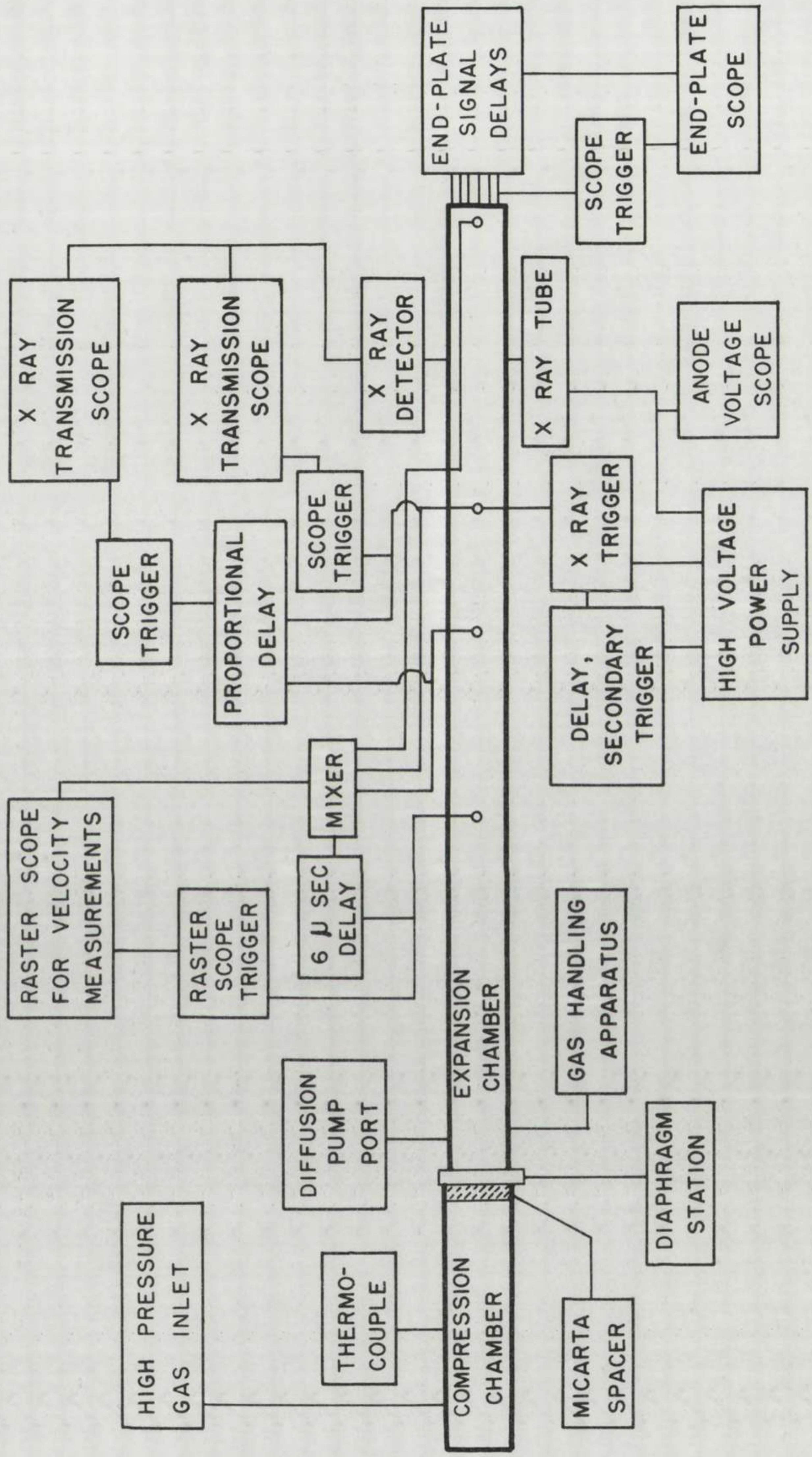
END-PLATE SIGNAL DELAYS
END-PLATE SCOPE
SCOPE TRIGGER
SCOPE TRIGGER
X RAY TRANSMISSION SCOPE
X RAY TRANSMISSION SCOPE
X RAY DETECTOR
X RAY TUBE
ANODE VOLTAGE SCOPE
SCOPE TRIGGER
SCOPE TRIGGER
PROPORTIONAL DELAY
X RAY TRIGGER
HIGH VOLTAGE POWER SUPPLY
DELAY, SECONDARY TRIGGER
MIXER
RASTER SCOPE FOR VELOCITY MEASUREMENTS
RASTER SCOPE TRIGGER
6 μ SEC DELAY
GAS HANDLING APPARATUS
EXPANSION CHAMBER
DIFFUSION PUMP PORT
DIAPHRAGM STATION
HIGH PRESSURE GAS INLET
THERMO-COUPLE
COMPRESSION CHAMBER
MICARTA SPACER

were used. The diaphragm material used in these experiments usually consisted of one to four sheets of 0.005 in. mylar. For the strongest shocks, 0.032 in. copper plates variously scribed 0.010 in. to 0.015 in. deep were used. In all experiments helium driver gas pressure was raised until the diaphragm ruptured spontaneously. Bursting pressures varied from 80 to 600 psig. Helium was used instead of hydrogen to eliminate shock perturbations due to burning at the contact surface.

The expansion chamber was a circular cross-section tube, 3 in. i.d. and 15 ft in length. The two inch diameter port for the diffusion pump was located as close as possible to the diaphragm station to minimize the perturbation caused by the small departure from a cylindrical tube. The expansion chamber could be evacuated to a pressure of 0.4 micron of Hg as measured with a McLeod gage. The leak rate, measured prior to every experiment, was usually less than 1 micron in 5 min, and was never more than 1 micron of Hg in 3 min. Since ten minutes was the normal time from the start to completion of an experiment, the impurity level was negligible. The x ray station was located 14 ft from the diaphragm. The demountable x ray windows consisted of 0.005 in. beryllium mounted on 2 in. diameter brass plugs so that the beryllium was flush with the inside wall of the shock tube. The beryllium windows were attached to the brass plugs with A-1 epoxy cement. A fan shaped x ray beam passed through the lower window, 0.030 in. by 0.500 in., into the shock tube, out the upper window, 0.030 in. by 1.500 in., and on to the x ray detector, which will be discussed later.

were used. The [illegible]

consisted of [illegible]

[illegible]

[illegible]

[illegible]

[illegible]

elements [illegible]

The [illegible]

and [illegible]

was [illegible]

the [illegible]

[illegible]

[illegible]

[illegible]

more than [illegible]

[illegible]

[illegible]

[illegible]

[illegible]

[illegible]

[illegible]

[illegible]

[illegible]

[illegible]

Ionization probes[12] were used to detect arrival of the shock wave at various points along the shock tube. A probe consisted of two wires, exposed to the flow with an electrical potential between them. As the ionized particles in the shock front passed the wires, a current flowed between the wires which caused a voltage across a resistor in an attached circuit. This voltage signal was amplified and used as a velocity or trigger signal. The probes were modified by the addition of a 0.5 mm step which projected into the flow immediately downstream of the electrodes. A shock reflecting from this step produces a higher temperature and therefore more ionization, which results in a larger probe signal. This design markedly improved the performance of the ionization probes in the lower portion of the velocity range studied.

For velocity measurements the signals from the four velocity probes had to be fed to a single input at the raster scope. This was accomplished with a mixer. The mixer consisted of four cathode follower circuits with a common cathode resistor, giving four grid inputs and one cathode follower output to the raster scope. The distance between the first and last velocity probe was 1.114 m; the x ray station was located midway between the last two probes. Shock wave attenuation, measured for each experiment, amounted to approximately 1% per meter. The shock velocity at the x ray station was inferred with an accuracy of 0.2% from a curve of average velocity between successive pairs of probes vs position in the tube. This measurement was quite important since the no-reaction temperature depended strongly upon it. A 1% error in the shock velocity would result in a 1.5% to 1.9% error in the no-reaction temperature, depending upon the shock strength and initial composition.

[illegible]

at [illegible]

exposed to the flow [illegible]

[illegible] particles in the [illegible]

between the [illegible]

circuit. [illegible]

magnet. [illegible]

bracket [illegible]

check [illegible]

bars to [illegible]

ally [illegible]

of the cylinder [illegible]

[illegible]

The x ray power supply consisted of a 2.5 μf condenser bank that could be discharged through a triggered spark gap, a 5 000 ohm limiting resistor, and the x ray tube to ground. The condenser bank was normally charged to 28.2 kv. With x ray tube currents of approximately 0.3 amp, the x ray anode voltage was 25 kv due to voltage drops across the spark gap and the current limiting resistor. The initial x ray trigger, as shown on Fig. 1, was split and one part delayed 500 μsec. This delayed signal triggered a second spark gap which shorted the high voltage capacitor bank to ground through a 500 ohm current limiting resistor.

The cathode of the x ray tube consisted of a spiral filament of twenty turns of 0.020 in. tungsten wire. The defocusing obtained with the spiral filament cathode made it possible to draw higher x ray currents without high voltage breakdown or erosion of the anode. In addition very reproducible x ray signals were obtained when the x ray tube was pulsed.

The x ray detector consisted of a scintillator and a photomultiplier tube. The scintillator used was polystyrene containing 1% p - terphenyl, 0.05% α - phenylnaphthyloxazole, and 0.03% zinc stearate. It was attached to the photomultiplier tube with epoxy cement. The scintillator, as shown in Fig. 2, was given a very thin, slightly transparent, evaporated coat of aluminum on the exposed surfaces to increase the light gathering efficiency. The increase of light to the photomultiplier from the scintillator design and the increased x ray tube current produced saturation in the photocathode and the later amplification dynodes in the previous photomultiplier tube. A modified RCA 2020 photomultiplier tube with only 7 amplification stages eliminated these difficulties.

Fig. 2. Drawing of the aluminum coated scintillator mounted on the photomultiplier tube.

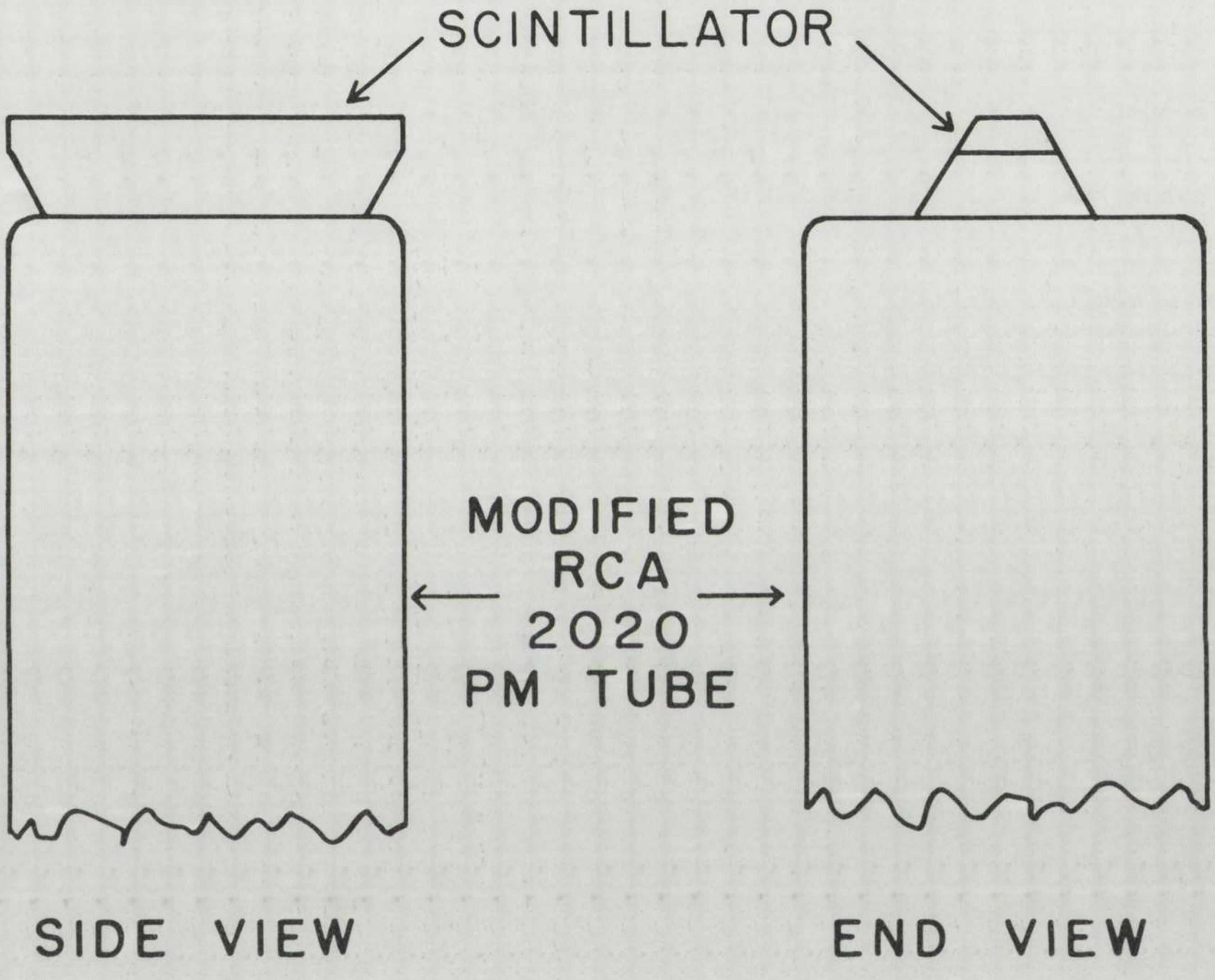
SCINTILLATOR
MODIFIED
RCA
2020
PM TUBE
SIDE VIEW
END VIEW

During an experiment two oscilloscope traces of the x ray signal were obtained simultaneously. One showed the full x ray signal, including the zero transmission level. The other, at a five times faster sweep speed, showed only the shock front and dissociation region. Records of the anode voltage of the x ray tube and shock velocity signals were also obtained on every experiment. Monitor traces were obtained after each experiment by again pulsing the x ray tube. These monitor traces were used in the data reduction procedure to establish what the x ray output would have been in the absence of the shock.

It was impossible to place an ionization probe close enough to the x ray station to trigger directly the fast sweep, x ray transmission scope. A proportional delay was developed by W. W. Steger which gave a trigger pulse when the shock was approximately 30 mm in front of the x ray station regardless of the shock velocity. This delay utilized the time interval between signals from the two velocity probes directly in front of the x ray station in generating this delayed trigger pulse.

In order to determine the magnitude of the shock front curvature and/or tilt an end-plate of 3/4 in. thick steel was fitted with 6 ionization probes ground flush with the end-plate. Of the 6 probes, 4 were arranged on one diameter and 3 on a diameter normal to the first--a probe in the center was common to both diameters. Four of these probes were located on a circle with a radius of 1.44 in., and one probe was located 1.13 in. from the center. Signals from these probes were delayed from 1 to 6 μsec at 1 μsec intervals and displayed on an oscilloscope.

Calibration of the x ray absorption of Xe and O_2 gases was accomplished in a test cell having the same cross-sectional area as the shock tube. The beryllium windows used for the experiment were used in the calibration setup. The x ray beam was monitored in order that the initial transmission in the test cell did not vary during calibration. Xenon or oxygen was admitted to the test cell and the new transmission as well as the gas pressure were recorded. Calibration runs were made at x ray anode voltages of 25 kv and the results reproduced within 0.6% in transmission. The x ray anode voltage during shock experiments was held at 25 ± 0.1 kv. Separate calibration experiments and calculations were made which showed that in the worst possible case a 0.1 kv variation in the x ray anode voltage would have produced only a 0.2% change in the final density, an uncertainty small compared to other errors.

Absorption curve A - C in Fig. 3 was obtained for xenon and curve A - B for oxygen. Under the conditions of this experiment the measured absorption coefficient of O_2 was a constant; this fact was used in calculating the absorption curve for mixtures of Xe and O_2. Essentially, the absorption curves for the Xe - O_2 mixtures were calculated by adding the x ray absorptions due to the partial densities of the components of the mixture. A more detailed description of the procedure follows. The density, corresponding to an experimental point E in Fig. 3, from the xenon calibration curve is multiplied by the ratio of the total mixture density to the xenon density. This gives point F with an abscissa corresponding to the total mixture density and an

Fig. 3. X ray absorption curves for Xe, O_2 and 30% Xe - 70% O_2 mixture.

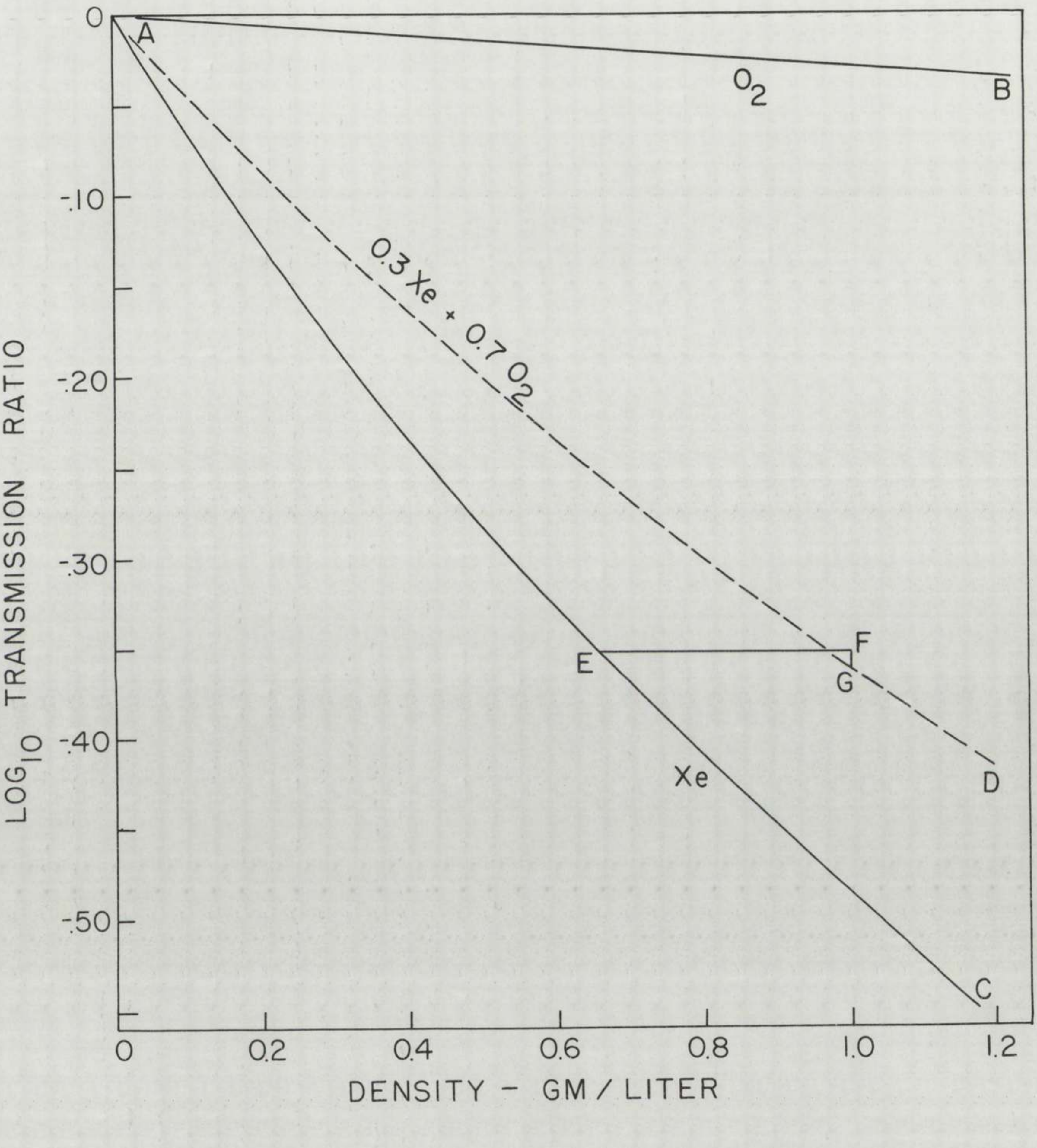

0
-.10
-.20
-.30
-.40
-.50
LOG10 TRANSMISSION RATIO
A
O2
B
0.3 Xe + 0.7 O2
E
F
G
D
Xe
C
0
0.2
0.4
0.6
0.8
1.0
1.2
DENSITY - GM / LITER

ordinate representing the absorption of the Xe present. The ratio of oxygen density to xenon density in the mixture is then multiplied by the absorption coefficient for oxygen and the density of xenon at point E. This gives the absorption of the oxygen present represented by the distance F - G in the same figure. Point G is then one point on the absorption curve for the Xe - O_2 mixture. This process is repeated using all the xenon calibration points. This defines the curve A - D, the absorption curve for a 30% Xe - 70% O_2 mixture.

The xenon used in the experiment was obtained from the Monsanto Chemical Company, Mound Laboratory, Miamisburg, Ohio and was 99.8% pure. It had an unnatural isotopic composition as follows: xenon 131--10.7%; xenon 132--16.9%; xenon 134--28.9%; and xenon 136--43.5%. The oxygen used was ordinary Linde tank grade, 99.8% pure. None of its impurities could have resulted in an observable change in the final rate values, since the impurities have been found to be less efficient than O_2 or O in producing dissociation[1].

Profiles representing the change in density as a function of distance behind the shock front were derived from photographs of oscilloscope traces of the amplitude of the detected x ray signal as a function of time. Pulse height as a function of distance from a reference point on the trace and a distance-time relationship for the film were read from the records using an optical comparator. This information was combined, by means of a simple IBM 704 code, with calibration, pertinent shock wave parameters and monitor trace data to yield the desired profiles.

The error in measured densities was usually less than 1%. However, in the oxygen rich mixtures it became necessary to go to lower initial pressures to obtain shocks strong enough to produce measurable dissociation. The lower initial density and smaller changes in transmission across the shock led to a larger but still less than 2% error in measured density as determined by a comparison of the observed and calculated equilibrium densities.

IV. Results

A total of sixteen experiments were performed with varying composition, initial temperature and pressure, and degree of dissociation. Details of the compositions, shock velocities, shock temperatures, and degrees of dissociation attained are reported in Table I. Typical x ray records from experiment No. 14 in Table I are shown in Figs. 4 and 5. Figure 4 shows the entire x ray signal and Fig. 5 is a delayed expanded signal showing in more detail the region in the vicinity of the front of the same shock. The mixture was 95% Xe - 5% O_2 at an initial pressure of 19.9 mm Hg. The shock velocity was 1.229 mm/μsec. Figure 6 is a plot of the density profile calculated from these two records. The circles represent densities derived from the record in Fig. 4, and the X's are points from the record in Fig. 5. The solid line is the profile calculated using the rates determined by this work. The dotted lines represent a ± 15% change in the Xe rate. The no-reaction density is observable in Figs. 4 and 5 as the start of the trace immediately following the abrupt change in x ray signal due to the shock. As can be seen from

The error in measured densities was generally less than 1%. However in the oxygen rich mixtures it became necessary to go to lower initial pressures to obtain marks strong enough to measure accurately; accordingly the lower initial density and smaller changes in density across the shock led to a larger but still less than 2% error in measured density as determined by a comparison of the observed and [illegible] densities.

IV. Results

A total of sixteen experiments were performed with various compositions, initial temperature and pressure, and degree of dissociation. Details of the composition, shock velocities, [illegible] and the degrees of dissociation obtained are reported in Table I. Typical data obtained from experiment No. [illegible] in Table I are shown in Figs. 4 and 5. Figure 4 shows the entire x-ray signal and Fig. 5 is a [illegible] trace showing in more detail the region in the vicinity of the [illegible] of the same shock. The mixture was [illegible] at an initial pressure of [illegible] mm Hg. The shock velocity was [illegible] of the density profile calculated from these two records [illegible] represent densities obtained from the record in Fig. 4, and the [illegible] points from the record in Fig. 5. The solid line is the profile [illegible] fitted using the rates calculated by this method. The [illegible] represent a [illegible] change in the [illegible]. The [illegible] presented in Figs. 4 and 5 [illegible] the abrupt change in x-ray signal due to the shock [illegible]

TABLE I

Resume of Experiments

No.	Composition % Xe	% O_2	T_o °C	P_o mm Hg.	Shock Velocity mm/μsec	% Dis. of O_2	No-Reaction Temperature °K
1	30.11	69.89	25.6	20.0	1.576	0.9	2710
2	30.11	69.89	27.3	10.0	1.814	8.9	3436
3	30.11	69.89	26.8	10.3	1.858	11.0	3580
4	30.11	69.89	25.8	9.9	2.001	17.1	4062
5	50.02	49.98	28.0	20.2	1.757	14.7	4520
6	50.02	49.98	26.0	20.1	1.548	7.0	3621
7	50.02	49.98	27.6	20.2	1.498	5.6	3422
8	85.00	15.00	26.1	20.1	1.315	34.2	4459
9	85.00	15.00	25.8	19.9	1.339	37.6	4609
10	85.00	15.00	26.0	20.1	1.318	34.6	4478
11	85.00	15.00	25.3	30.4	1.239	22.8	3998
12	95.01	4.99	24.4	20.0	1.432	99.5	6014
13	95.01	4.99	23.5	20.1	1.340	97.3	5300
14	95.01	4.99	26.0	19.9	1.229	81.9	4510
15	95.01	4.99	24.3	29.9	1.179	70.7	4173
16	95.01	4.99	25.2	18.9	1.267	90.1	4774

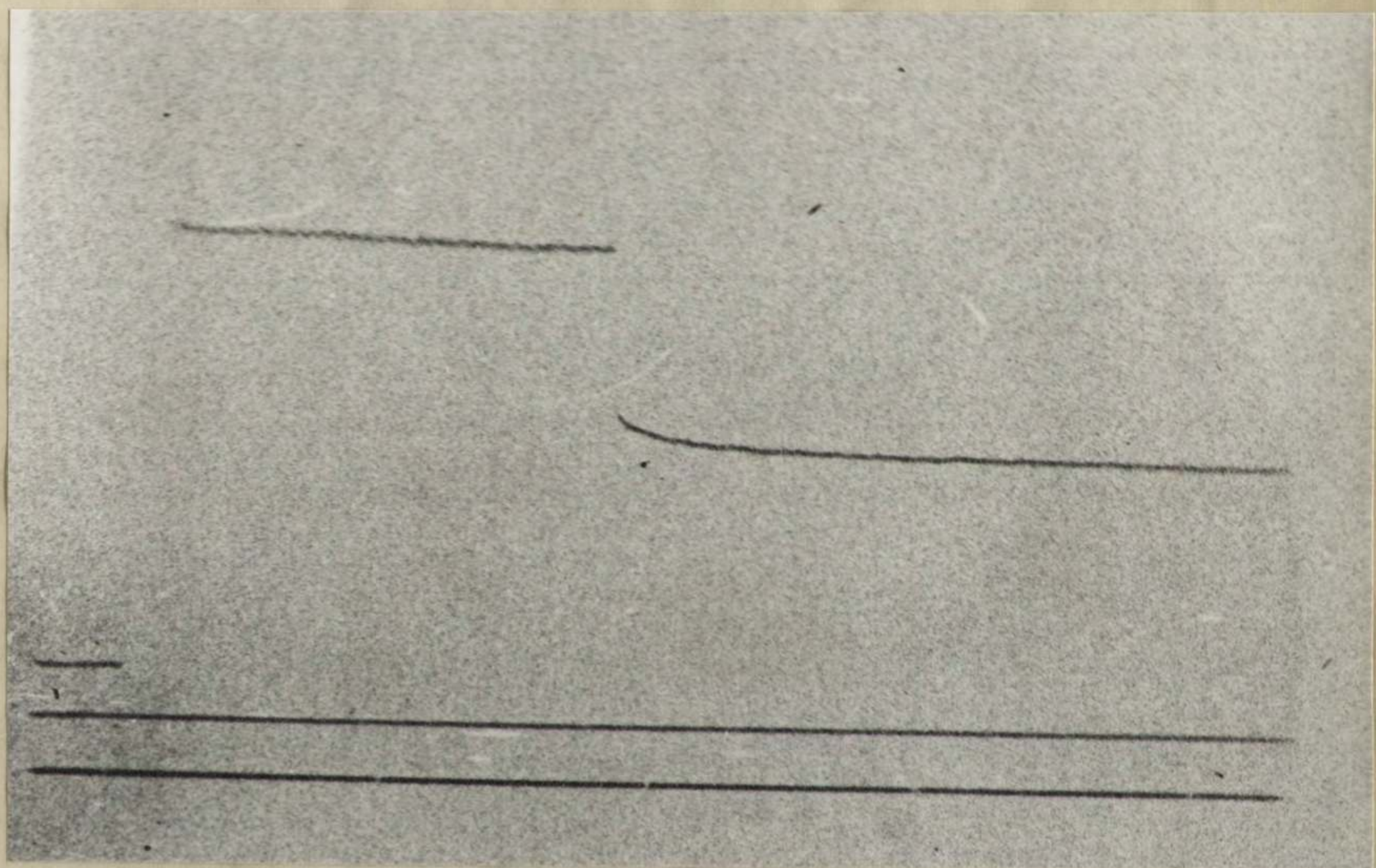

Fig. 4. A typical oscilloscope record of the change in x ray transmission across a shock in a 95% Xe - 5% O_2 mixture at an initial pressure of 1.99 cm Hg. The three sweep traces from top to bottom are the x ray signal, a base line, and 100 μsec timing marks. Shock velocity was 1.229 mm/μsec.

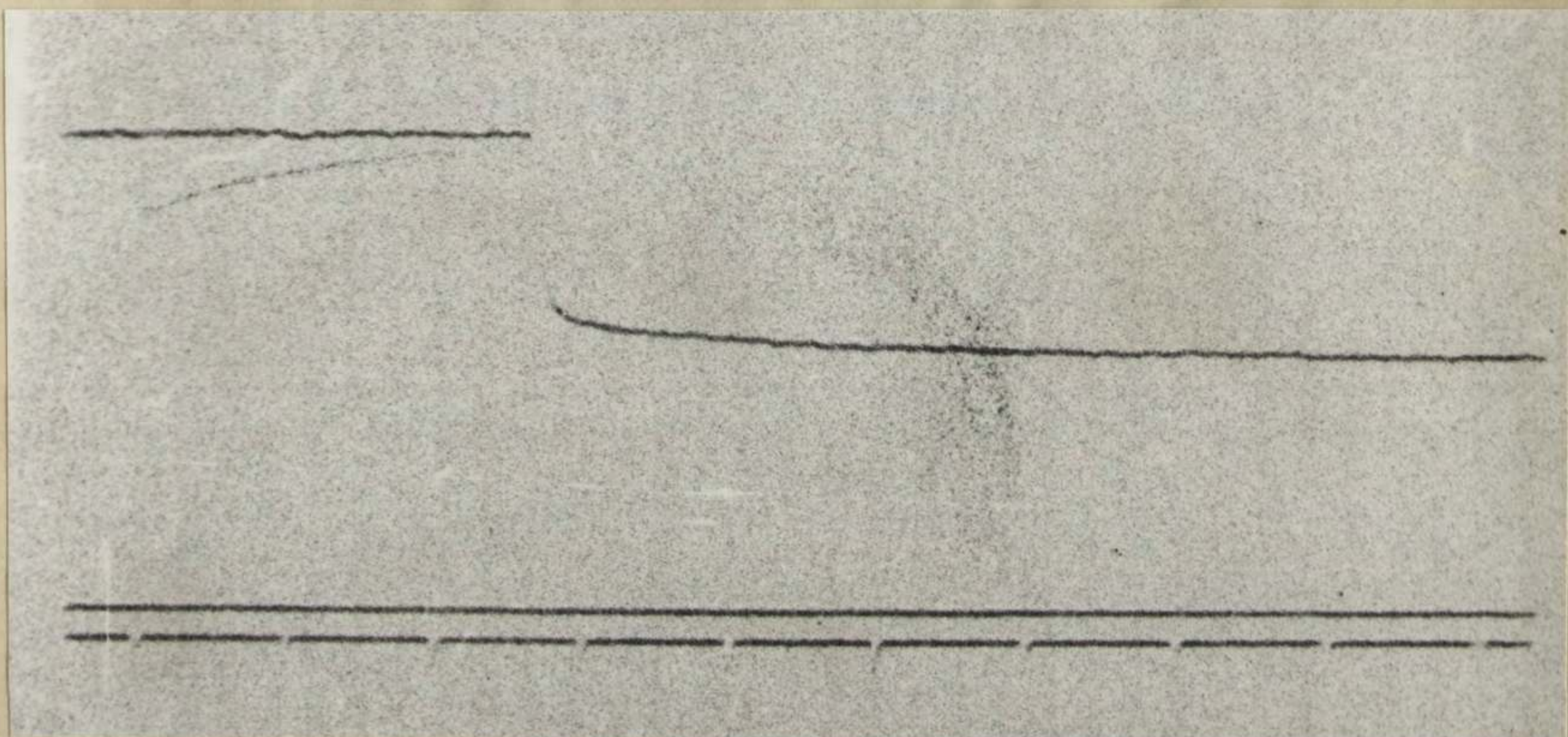

Fig. 5. Same signal as Fig. 4, except that a faster sweep speed was used - 10 μsec timing marks. The base line is not displaced in this record.

Fig. 6. Plot of density profile. Circles represent density points from record in Fig. 4, and X's are points from record in Fig. 5. Solid line is profile using rates which fit all the experimental density profiles. The dotted lines represent a ± 15% change in the Xe rate.

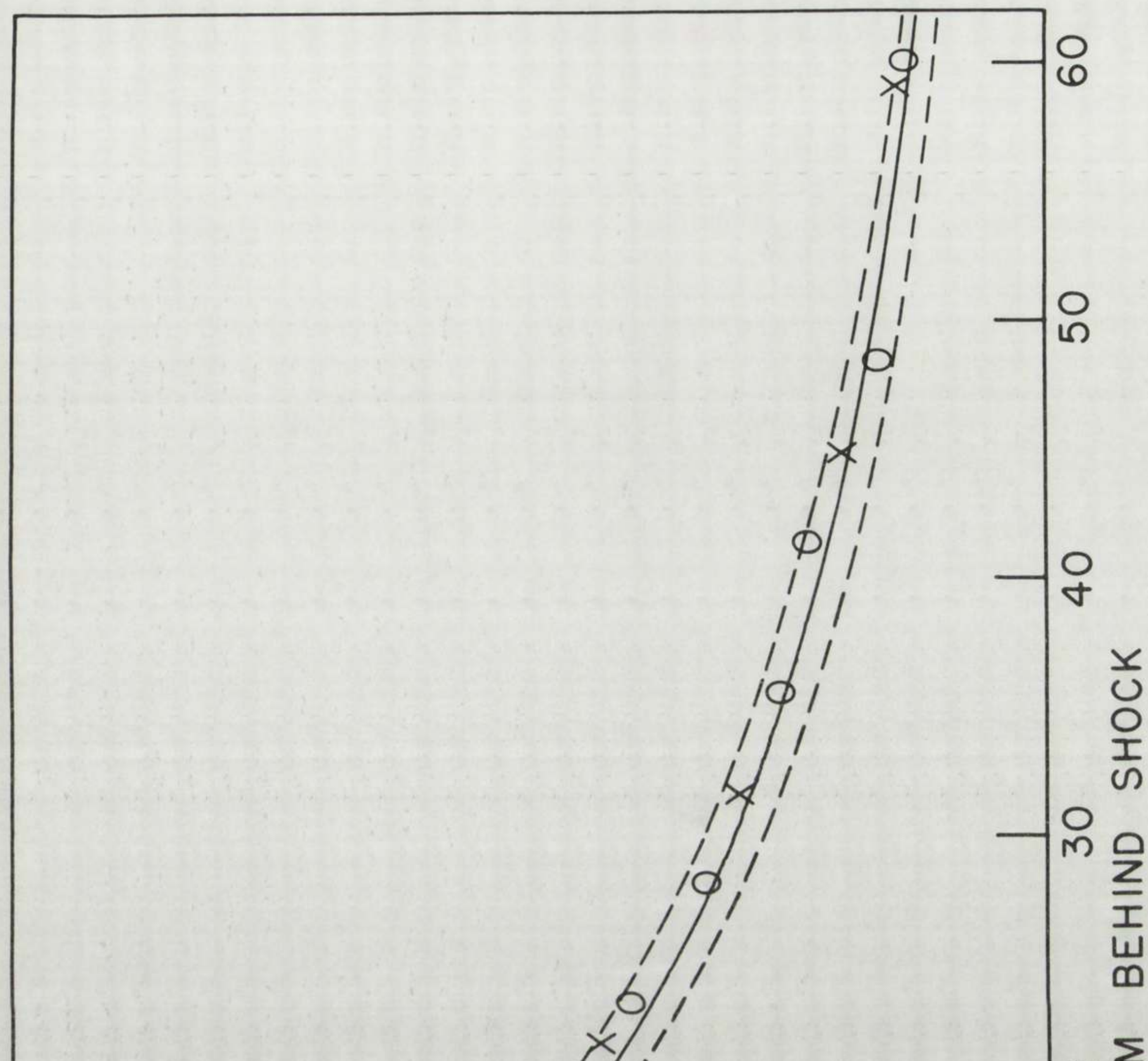
NO REACTION DENSITY / DENSITY
1.00
.95
.90
.85
.80
MM BEHIND SHOCK
0
10
20
30
40
50
60

Fig. 6, this no-reaction point is 3.8 mm behind the shock front. This distance varied from 2 mm to 8 mm and was produced mainly by vibrational relaxation, but included transit time across the beam and response time of the electronic circuitry. End-plate measurements have eliminated the possibility of deviations from a planar shock contributing to this delay. At no time did wave curvature and/or tilt cause the wave front to deviate from a diametral plane by as much as the x ray slit width--3/4 mm. Normally these effects were less than half the slit width.

A set of rate coefficients, k_{r_i}, was found with which it was possible to fit all 16 experiments. The recombination rates for each of the third-bodies, Xe, O_2, O, as determined in this experiment are listed below:

$$k_{rXe} = 4.7 \times 10^{17}\ T^{-1} \quad \pm 15\%$$

$$k_{rO_2} = 1.6 \times 10^{18}\ T^{-1} \quad \pm 20\%$$

$$k_{rO} = 4.8 \times 10^{18}\ T^{-1} \quad \pm 20\% \qquad cc^2,\ mole^{-2},\ sec^{-1}.$$

Analysis of the data obtained in this work revealed that the 3000°K - 6000°K temperature range covered was insufficient to do more than establish the limits of -1/2 to -2 for the temperature exponents, m_i. Therefore they were arbitrarily set equal to -1.0. The error limits were obtained by varying successively the recombination rates until the calculated density profiles deviated significantly from the experimental density profiles as shown in Fig. 6 for k_{rXe}. This procedure is legitimate because each of the three dissociation reactions predominates over the other two for some range of composition and extent of reaction.

V. Comparison with Other Results

The recombination rate coefficients evaluated at 3500°K reported by different investigators for various third bodies are presented in Table II. Camac and Vaughan[3] utilized an ultraviolet light absorption technique to observe the rate of disappearance of O_2 behind shock waves in Ar-O_2 mixtures. From this information and knowledge of initial conditions and shock velocity, the reported rate coefficients were obtained. According to their report recombination reactions were not included in their calculations. This omission would tend to cause their rates to be too low. It should be noted that the value of 8 reported by Camac and Vaughan for the third body efficiency* of O relative to O_2 is in substantial disagreement with the value of 3 obtained here. Since our value was obtained by a detailed analysis of the entire dissociation process from the onset of reaction to equilibrium including the effects of recombination, I suggest that it is probably the more reliable result.

Byron[1], using an optical interferometer and drum camera, measured the time required for half the density change due to dissociation to occur. From this he deduced rates of dissociation. He worked with both pure oxygen and oxygen diluted with argon. Recombination effects were not included in his calculations. Therefore, his results also are probably somewhat low. However the third body efficiency of O relative to O_2 reported by Byron is not in serious disagreement with my value. See Appendix A for the evaluation of Byron's recombination rates from his published data.

*In this paper the relative efficiency of one third body to another will be defined as the ratio of their respective rate coefficients at 3500°K.

V. Comparison with Other Results

The recombination rate coefficients evaluated at 7000°K reported by different investigators for various third bodies are presented in Table II. Camac and Vaughan[9] utilized an ultraviolet light absorption technique to observe the rate of disappearance of O_2 behind shock waves in Ar-O_2 mixtures. From this information and knowledge of initial conditions and shock velocity, the reported rate coefficients were obtained. According to their report recombination reactions were not included in their calculations. This omission would tend to cause their rates to be too low. It should be noted that the value of R reported by Camac and Vaughan for the third body efficiency* of O relative to O_2 is in substantial disagreement with the value of 3 obtained here. Since our value was obtained by a detailed analysis of the entire dissociation process from the onset of reaction to equilibrium including the effects of recombination, I suggest that it is probably the more reliable result.

Byron[6], using an optical interferometer and drum camera, measured the time required for half the density change due to dissociation to occur. From this he deduced rates of dissociation. He worked with both pure oxygen and oxygen diluted with argon. Recombination effects were not included in his calculations. Therefore, his results also are probably somewhat low. However, the third body efficiency of O relative to O_2 reported by Byron is not in serious disagreement with ours. See Appendix A for the evaluation of Byron's recombination rates from his published data.

*In this paper the relative efficiency of one third body to another will be defined as the ratio of their respective rate coefficients at 7000°K.

TABLE II

Recombination Rates of Oxygen at 3500°K

Investigator	Method	Type Third Body	k_r, $cc^2 mole^{-2} sec^{-1}$ at 3500°K
This paper	x ray	O_2	4.6×10^{14}
		Xe	1.3×10^{14}
		O	1.4×10^{15}
Camac & Vaughan	Ultra-violet	O_2	1.6×10^{14}
		Ar	5.2×10^{13}
		O	1.3×10^{15}
Byron	Light-interferometer	O_2	4.8×10^{14}
		Ar	4.5×10^{13}
		O	9.9×10^{14}
Matthews	Light-interferometer	O_2	8×10^{14}
Losev	Ultra-violet	O_2	2×10^{14}
Chesick & Kistiakowsky	x ray	O_2 - Xe	2×10^{14}

Matthews[2] obtained Mach-Zehnder interferograms of shocks in pure oxygen. From these he derived a density vs distance profile behind the shock. He then compared the experimental profiles with profiles calculated using a collision theory rate equation. He was the first to consider both dissociation and recombination in the analysis of his data. Matthews was unable to measure the rate of dissociation caused by the O_2 - O collisions, so for his calculation he used Byron's work to obtain information concerning O to O_2 third body efficiency ratio. If the O to O_2 efficiency ratio were larger than that given by Byron, as reported by both Camac and Vaughan and this work, the rate quoted by Matthews would tend to be too high.

Losev[4] employed ultra-violet absorption to measure the temperature distribution behind shocks in pure oxygen. He worked with strong shocks, 2.7 - 3 mm/μsec, and a low initial pressure of 7.6 mm of Hg. Under these conditions the results of Camac and Vaughan suggest that he was probably observing vibrational relaxation and dissociation simultaneously. The rate quoted in Table II was taken from a graph and is probably only accurate to 50%.

The rate reported by Chesick and Kistiakowsky[13] is the average of only two experiments. There was no mention of any attempts to separate the rates of the different third bodies; so this rate is probably an average of effects of all third bodies present. A mixture of 25.1% Xe - 74.9% O_2 was used in their experiment.

VI. Conclusions

The combination of the x ray densitometer and an IBM 704 computer for data analysis has been shown to be adaptable to a study of the dissociation rate of oxygen. With a single set of rate coefficients it was possible to fit the density profiles of sixteen experiments in which the composition, initial pressure, and degree of dissociation were varied. Fair agreement with previous work is obtained. It is felt that this investigation demonstrates the feasibility of using this method in kinetic studies of other gases.

VI. Conclusions

The combination of the x ray densitometer and an IBM 704 computer for data analysis has been shown to be adaptable to a study of the dissociation rate of oxygen. With a single set of rate coefficients it was possible to fit the density profiles of sixteen experiments in which the composition, initial pressure, and degree of dissociation were varied. Fair agreement with previous work is obtained. It is felt that this investigation demonstrates the feasibility of using this method in kinetic studies of other gases.

Appendix A

The following calculations were made in obtaining the recombination rates attributed to Byron[1]. His results were reported in terms of the following equation and constants:

$$\frac{D[O]}{D\,t} = 2\,(\rho/m)^2\, D^2\, \bar{v}\, \exp\,(-T_{DIS}/T) \left\{ K_1\, C_1^2\, \frac{(1-\alpha)^2}{n_1\,!}\, (T_{DIS}/T)^{n_1} \times 1.052 \right.$$

$$+ K_2\, \frac{C_1(1-C_1)(1-\alpha)}{n_2\,!}\, (T_{DIS}/T)^{n_2}$$

$$\left. + K_3\, C_1^2\, (1-\alpha)\, (T_{DIS}/T) \times 1.304 \right\} \qquad (1)$$

$D = 3.64 \times 10^{-8}$ cm; $\bar{v} = (8\pi kT/\mu_{12})^{1/2}$; $\mu_{12} = m_{O_2}\, m_{Ar}/(m_{O_2} + m_{Ar})$;

$T_{DIS} = E_{DIS}/R$; $n_1 = 2.0$; $n_2 = 1.0$; $K_1 = 0.24$; $K_2 = 0.10$; $K_3 = 1.7$.

The concentrations of the three components Ar, O_2, and O are

$$[Ar] = \rho/m\,(1 - C) \qquad (2)$$

$$[O_2] = \rho/m\; C\,(1 - \alpha) \qquad (3)$$

$$[O] = 2\,\rho/m\; C\,\alpha\;, \qquad (4)$$

where C is the fraction by volume of O_2, α is the degree of O_2 dissociation, and m is the average weight per particle of gas mixture.

To obtain the dissociation rates one needs to put Eq. 1 in the following form:

$$\frac{1}{2}\frac{D[O]}{D\,t} = -\frac{D[O_2]}{D\,t} = k_{d_{Ar}}\,[Ar][O_2] + k_{d_{O_2}}\,[O_2] + k_{d_O}\,[O][O_2]\,. \tag{5}$$

Using the Eqs. 3, 4, and 5 for the concentrations of the three components and regrouping, Eq. 1 becomes

$$\begin{aligned}\frac{1}{2}\frac{D[O]}{D\,t} = {} & \chi_2\, D^2\, \bar{v}\, (T_{DIS}/T)\ \exp(-T_{DIS}/T)\ \ [Ar][O_2] \\ & + 1.052/4\ \chi_1\, D^2\, \bar{v}\ (T_{DIS}/T)^2\ \exp(-T_{DIS}/T)\ [O_2] \\ & + 1.304\ \chi_3\, D^2\, \bar{v}\ (T_{DIS}/T)\ \exp(-T_{DIS}/T)\ [O][O_2]\end{aligned} \tag{6}$$

From Eq. 6 one obtains the following relationships for the k_{d_i} .

$$k_{d_{Ar}} = \chi_2\, D^2\, \bar{v}\ (T_{DIS}/T)\ \exp(-T_{DIS}/T) \tag{7}$$

$$k_{d_{O_2}} = 1.052/4\ \chi_1\, D^2\, \bar{v}\ (T_{DIS}/T)\ \exp(-T_{DIS}/T) \tag{8}$$

$$k_{d_O} = 1.304\ \chi_3\, D^2\, \bar{v}\ (T_{DIS}/T)\ \exp(-T_{DIS}/T) \tag{9}$$

To obtain the dissociation rate, it is useful to put Eq. 1 in the following form:

$$\frac{1}{2}\frac{d[O]}{dt} = -\frac{d[O_2]}{dt} = k_{d_{Ar}}[Ar][O_2] + k_{d_{O_2}}[O_2]^2 + k_{d_O}[O][O_2] \qquad (5)$$

Using the Eqs. 3, 4, and 5 for the concentrations of the three components and rearranging, Eq. 5 becomes

$$\frac{1}{2}\frac{d[O]}{dt} = K_2 D^2 \bar{v} (T_{n12}/T) \exp(-T_{n12}/T) [Ar][O_2]$$

$$+ 1.0527/4 \, K_4 D^2 \bar{v} (T_{n15}/T)^2 \exp(-T_{n15}/T) [O_2]^2$$

$$+ 1.304 \, K_5 D^2 \bar{v} (T_{n16}/T) \exp(-T_{n16}/T) [O][O_2] \qquad (6)$$

From Eq. 6 one obtains the following relationships for the k_d:

$$k_{d_{Ar}} = K_2 D^2 \bar{v} (T_{n12}/T) \exp(-T_{n12}/T) \qquad (7)$$

$$k_{d_{O_2}} = 1.0527/4 \, K_4 D^2 \bar{v} (T_{n15}/T)^2 \exp(-T_{n15}/T) \qquad (8)$$

$$k_{d_O} = 1.304 \, K_5 D^2 \bar{v} (T_{n16}/T) \exp(-T_{n16}/T) \qquad (9)$$

Eqs. 7, 8, and 9 are now evaluated at 3500°K. These equations are all multiplied by Avogadro's Number to put them on a per mole basis.

$$k_{d_{Ar}} = 3.73 \times 10^{7}$$

$$k_{d_{O_2}} = 4.00 \times 10^{8}$$

$$k_{d_O} = 8.28 \times 10^{8} \qquad cc, mole^{-1}, sec^{-1}$$

Using the equilibrium constant for 3500°K, 8.36×10^{-7} moles/cc, and the dissociation rates, one obtains the following values for the recombination rates for the three third bodies.

$$k_{r_{Ar}} = 4.5 \times 10^{13}$$

$$k_{r_{O_2}} = 4.8 \times 10^{14}$$

$$k_{r_O} = 9.9 \times 10^{14} \qquad cc^{2}, moles^{-2}, sec^{-1}$$

REFERENCES

1. S. R. Byron, J. Chem. Phys. 30, 1380 (1959).

2. D. L. Matthews, Phys. Fluids 2, 170 (1959).

3. M. Camac and A. Vaughan, Avco Everett Research Lab., Research Report 84, AFBMD-TR-60-22.

4. S. A. Losev, Doklady Akad. Nauk S.S.S.R. 120, 1291 (1958) [Soviet Phys. - Doklady 120, 467].

5. R. E. Duff, Phys. Fluids 1, 242 (1958).

6. H. S. Glick and W. H. Wurster, J. Chem. Phys. 27, 1224 (1957).

7. R. E. Duff, J. Chem. Phys. 28, 1193 (1958).

8. H. Johnston, L. Savedoff, J. Belyer, Ohio State Project RF-316, TR-316-4.

9.. Selected Values of Chemical Thermodynamic Properties, Series III, Table 7, NBS (1947).

10. P. Brix and G. Herzberg, Can. J. Phys. 32, 110 (1954).

11. H. T. Knight and D. Venable, Rev. Sci. Instr. 29, 92 (1958)

12. H. T. Knight and R. E. Duff, Rev. Sci. Instr. 26, 257 (1955).

13. J. P. Chesick and G. B. Kistiakowsky, J. Chem. Phys. 28, 956 (1958).

REFERENCES

1. [illegible], J. Chem. Phys. 31, 1390 (1959).

2. D. L. [illegible], Phys. Fluids 2, 170 (1959).

3. M. Camac and A. Vaughan, Avco Everett Research Lab. Research Report 84, AFBMD TR-60-22.

4. S. A. Losev, Doklady Akad. Nauk S.S.S.R. 120, 1291 (1958) [Soviet Phys — Doklad. 120, 467].

5. R. E. Duff, Phys. Fluids 1, 242 (1958).

6. H. S. Glick and W. H. Wurster, J. Chem. Phys. 27, 1224 (1957).

7. R. E. Duff, J. Chem. Phys. 28, 1193 (1958).

8. H. Johnston, [illegible], [illegible], Ohio State Project 4-316, TR-316-1.

9. Selected Values of Chemical Thermodynamic Properties, Series III, Table 7, NBS (1954).

10. F. [illegible] and G. [illegible], J. Chem. Phys. 22, 140 (1954).

11. H. T. Knight and [illegible], Rev. Sci. Instr. 29, 92 (1958).

12. H. T. Knight and R. E. Duff, Rev. Sci. Instr. 26, 257 (1955).

13. W. F. [illegible] and G. B. Kistiakowsky, J. Chem. Phys. 28, 598 (1958).